ISBN: 978-3-95450-184-7 doi:10.18429/JACoW-IPAC2018-THPAF059

ULTRA COMPACT SYMPLECTIC SCHEME FOR FAST MULTI-PARTICLE TRACKING

K. Skoufaris*†, D. Pellegrini, Y. Papaphilippou, CERN, Geneva, Switzerland

Abstract

A versatile symplectic integration scheme has been developed in order to produce simplified versions of non linear lattices, preserving fundamental non-linear properties such as the detuning with amplitude and energy, in addition to the linear transport. The method has been applied to the LHC and benchmarked against tracking simulations with Sixtrack. This reduced lattice is made available as a refined replacement of the simple rotation matrix often used in multi-particle studies requiring a fast beam transport routine.

INTRODUCTION

The great computational time needed to track a distribution of particles in a ring is one of the common limitations encountered in beam dynamics simulations. The most common solution is to use an element-by-element tracking through a symplectic integration scheme [1, 2]. An alternative method for fast multi-particle symplectic tracking is presented in this paper.

The proposed method that is close to the mentality of an extensive use of the Baker–Campbell–Hausdorff formula reproduces all the linear characteristics of the machine and at the same time retains a certain accuracy for the non-linear ones by using the least possible elements. The resulted transfer map (effective lattice) that describes the studied machine, in our case the LHC lattice, is symplectic and can be adjusted to fit the needs of other rings.

LINEAR PART

In the ultra relativistic limit ($\beta_{\text{rel}} \rightarrow 1$), the Hamiltonian at the linear sections (drifts, dipoles and quadrupoles, neglecting edge effects) is given by $\mathcal{H}_{\text{lin}} = V_{\text{lin}}(q; s) + \sum_q \frac{P_q^2}{2(\delta+1)}$. The linear sections in the effective lattice are periodic with period L (as in the target lattice) and the energy spread in one revolution is constant $\delta = \text{const}$ (no RF cavities are considered). Thus, the betatron motion is described by the Hill's equation $Q'' + k(s)\, Q = 0$ where, $k(s) = K(s)/(\delta+1)$ and $k(s+L) = k(s)$. The solution of the linear uncoupled transverse motion can be described by:

$$\mathbf{Z}_{Q_f} = \mathcal{M}^{(Q,Q')} \mathbf{Z}_{Q_i} \quad , \tag{1}$$

where $\mathbf{Z}_Q$ is a vector containing the dynamic variables (Q, Q'), $\mathcal{M}^{(Q,Q')}$ is the known 2×2 rotation matrix that transforms the dynamic variables from some initial (i) lattice point to a final one (f). In order to use the conjugate variables q and P_q, the transformation $q = Q$ and $Q' = \frac{\partial \mathcal{H}}{\partial P_q} \rightarrow P_q = Q'(\delta+1)$ for the transverse motion is used. As said, during one revolution $\Delta\delta = 0$ and so, $\omega \equiv \delta + 1 = \text{const}$. Thus, the transformation $\mathbf{Z}_Q \rightarrow \mathbf{Z}_q$ is an extended symplectic transformation [3] and is given by:

$$\mathbf{Z}_q = \mathbf{J}\, \mathbf{Z}_Q \Rightarrow \begin{pmatrix} q \\ P_q \end{pmatrix} = \begin{pmatrix} 1 & 0 \\ 0 & \omega \end{pmatrix} \begin{pmatrix} Q \\ Q' \end{pmatrix} \quad , \tag{2}$$

where $\mathbf{J}$ is the Jacobian of the transformation. For the new set of dynamic variables (q, P_q) the rotation in Eq. (1) is transformed according to the relation $\mathcal{M}^{(q,P_q)} = J \mathcal{M}^{(Q,Q')} J^{-1}$.

The map $\mathcal{M}^{(q,P_q)}$ describes only the betatron motion. In order to add the contribution from the dispersion, the transformation of the $\mathbf{Z}_q$ is given by:

$$\begin{pmatrix} q \\ P_q \end{pmatrix}_f = \begin{pmatrix} \mathcal{M}_{1,1}^{(q,P_q)} & \mathcal{M}_{1,2}^{(q,P_q)} \\ \mathcal{M}_{2,1}^{(q,P_q)} & \mathcal{M}_{2,2}^{(q,P_q)} \end{pmatrix} \begin{pmatrix} q \\ P_q \end{pmatrix}_i + \begin{pmatrix} \mathcal{M}_{1,3}^{(q,P_q)} \\ \mathcal{M}_{2,3}^{(q,P_q)} \end{pmatrix} (\omega - 1) \, . \tag{3}$$

The unknown elements for the moment are the $\mathcal{M}_{1,3}^{(q,P_q)}$ & $\mathcal{M}_{2,3}^{(q,P_q)}$. Since the optical functions of the target lattice are known, the expressions of the $\mathcal{M}_{1,3}^{(q,P_q)}$ & $\mathcal{M}_{2,3}^{(q,P_q)}$ can be calculated by making use of the dispersion functions (D_q, D_{P_q}). Interpreted as the motion of a special particle with $\delta = 1$, D_q and D_{P_q} can be transformed according to Eq. (3) by making the following changes $q \rightarrow D_q$, $P_q \rightarrow D_{P_q}$ and $\omega \rightarrow 2$. Solving with respect to $\mathcal{M}_{1,3}^{(q,P_q)}$ & $\mathcal{M}_{2,3}^{(q,P_q)}$, a general expression is obtained. For completeness, the elements of the matrix $\mathcal{M}^{(q,P_q)}$ are the following ones:

$$\mathcal{M}_{1,1}^{(q,P_q)} = \sqrt{\frac{\beta_{q_f}}{\beta_{q_i}}} \left(Cos(\psi_q) + \alpha_{q_i} Sin(\psi_q) \right) \tag{4a}$$

$$\mathcal{M}_{1,2}^{(q,P_q)} = \frac{\sqrt{\beta_{q_f} \beta_{q_i}}\, Sin(\psi_q)}{\omega} \tag{4b}$$

$$\mathcal{M}_{1,3}^{(q,P_q)} = D_{q_f} - Dq_i\, \mathcal{M}_{1,1}^{(q,P_q)} - D_{P q_i}\, \mathcal{M}_{1,2}^{(q,P_q)}|_{\omega \rightarrow 2} \tag{4c}$$

$$\mathcal{M}_{2,1}^{(q,P_q)} = \omega \frac{(\alpha_{q_i} - \alpha_{q_f})\, Cos(\psi_q) - (1 + \alpha_{q_i} \alpha_{q_f})\, Sin(\psi_q)}{\sqrt{\beta_{q_f} \beta_{q_i}}} \tag{4d}$$

$$\mathcal{M}_{2,2}^{(q,P_q)} = \sqrt{\frac{\beta_{q_i}}{\beta_{q_f}}} \left(Cos(\psi_q) - \alpha_{q_f} Sin(\psi_q) \right) \tag{4e}$$

$$\mathcal{M}_{2,3}^{(q,P_q)} = D_{P q_f} - D_{q_i}\, \mathcal{M}_{2,1}^{(q,P_q)}|_{\omega \rightarrow 2} - D_{P q_i}\, \mathcal{M}_{2,2}^{(q,P_q)} \, , \tag{4f}$$

where β and α are the Courant–Snyder parameters of the lattice and ψ is an effective phase advance. All the optical functions are the same or similar to the ones of the target lattice and they are obtained by using the Methodical Accelerator Design program [4]. If the study is not performed for the ultra relativistic limit, the $\mathcal{M}_{1,3}^{(q,P_q)}$ & $\mathcal{M}_{2,3}^{(q,P_q)}$ elements must be multiplied by β_{rel} [5]. In order to capture the linear chromatic aberration, it should be $\psi = \mu_{i \rightarrow f} + 2\, \pi \xi_{N_{i \rightarrow f}}\, \delta$ where,

* also at University of Crete, Heraklion, Greece
† Corresponding author; Email address: kyriacos.skoufaris.at.cern.ch

ISBN: 978-3-95450-184-7 doi:10.18429/JACoW-IPAC2018-THPAF059

$\mu_{i\to f}$ is the phase advance from s_i to s_f and $2\,\pi\xi_{N_{i\to f}}\,\delta$ is the contribution of the natural chromaticity ξ_N from s_i to s_f.

In order to describe the longitudinal motion and its coupling with the bending plane in a symplectic form, a rescaled set of longitudinal variables (λ, δ) must be used. The longitudinal displacement l and its conjugate variable δ are transformed according to Eq. (2) with the following changes $Q \to \delta$, $Q' \to l$, $q \to \widetilde{\delta}$ and $P_q \to \lambda$. The new symplectic set of the transverse and longitudinal variables is $(q, P_q, \lambda, \delta)$. In such a way, additionally to Eq. (4), the evolution of the longitudinal variables is given by:

$$\lambda_f = \lambda_i + \left(\mathcal{M}_{1,3}^{(q,P_q)}\mathcal{M}_{2,1}^{(q,P_q)} - \mathcal{M}_{1,1}^{(q,P_q)}\mathcal{M}_{2,3}^{(q,P_q)}\right) q_i + \left(\mathcal{M}_{1,3}^{(q,P_q)}\mathcal{M}_{2,2}^{(q,P_q)} - \mathcal{M}_{1,2}^{(q,P_q)}\mathcal{M}_{2,3}^{(q,P_q)}\right) P_{q_i} + \left(D_{q_f}\mathcal{M}_{2,3}^{(q,P_q)} - D_{P_{q_f}}\mathcal{M}_{1,3}^{(q,P_q)} + \frac{s_f - s_i}{\gamma_{rel}^2}\right)\delta_i \quad (5a)$$

$$\delta_f = \delta_i\ . \quad (5b)$$

Both of the 4D or 6D maps are symplectic representations of the linear motion in a lattice without coupling between the transverse plains.

NON-LINEAR PART

After every linear rotation a lumped non-linear kick is performed. In the case of the LHC effective lattice, combined thin sextupoles and octupoles are used. The 6D non-linear kick is given by:

$$x_f = x_i \quad (6a)$$

$$P_{x_f} = P_{x_i} - \frac{K_S}{2}(x_i^2 - y_i^2) - \frac{K_O}{2}\left(\frac{x_i^3}{3} - x_i y_i^2\right) \quad (6b)$$

$$y_f = y_i \quad (6c)$$

$$P_{y_f} = P_{y_i} + K_S x_i y_i + \frac{K_O}{2}\left(x_i^2 y_i - \frac{y_i^3}{3}\right) \quad (6d)$$

$$\lambda_f = \lambda_i \quad (6e)$$

$$\delta_f = \delta_i\ . \quad (6f)$$

with K_S and K_O being the normalized strengths of the sextupole and octupole respectively. For a better control of the chromaticity (linear and non-linear) and the tune shift with amplitude, different families of non-linear elements can be used. In view of having the smallest possible strengths (less non-linear perturbations to the particles motion), the non-linear kicks are placed in positions where the beta function is maximum. In addition, an extra mitigation of the lattice nonlinearities can be achieved if the phase advance ψ between the kicks of the same family is $\pi + 2\pi n$ with n being an integer (the so-called $-\mathcal{I}$ transformer). The tune shift with amplitude caused by the sextupolar kicks, despite being a second order effect, perturbs the footprint quite significantly. Knowing that it is sensitive to the phase advance between the kicks of the same family [5], locating them in phases of ψ equal to 3π or 5π minimizes the effect and preserves the $-\mathcal{I}$ transformation, at least for the reduced lattice. The values of the ψ, K_S and K_O can be automatically adjusted if they are associated with the known analytical formulas of the chromaticity and the tune shift with amplitude.

SIMULATION RESULTS

As a first check, footprints of the LHC lattice at flat bottom (450 GeV) and at flat top (6.5 TeV) energies, are compared with the ones from the relevant effective lattices. The very good reproduction of the footprints is shown in Fig. 1. The results for the full lattice and for the reduced one are plotted with red lines and blue dots respectively. The energy spread δ is set to zero while for the chromaticity ξ and the octupole current I_{octu}, the nominal values, for flat bottom and flat top energies, are used. The characteristic value G, seen in the following plots, corresponds to the total number of maps used for the construction of an effective lattice. For the flat

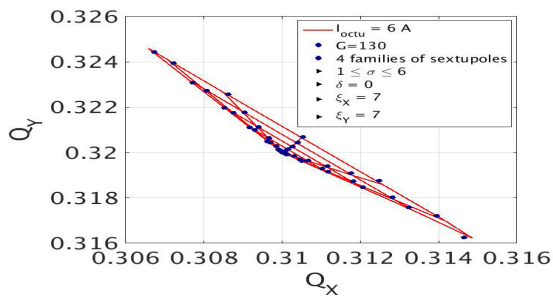

(a) Flat bottom

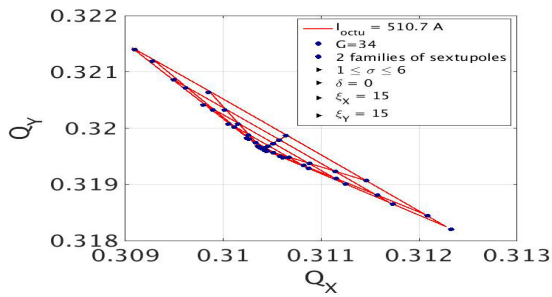

(b) Flat top

Figure 1: The red lines correspond to the footprint taken from the full lattice of the LHC and the blue dots to the one from the effective lattice.

bottom results in Fig. 1a, the octupoles have low current and so the opening of the footprint is significantly affected by the sextupoles. Therefore, four families of sextupoles are used in order to have a more refined control of the tune shift with amplitude. For flat top energies (see Fig. 1b), the octupoles are stronger (maximum I_{octu}). Consequently, the footprint is mainly formed by the octupoles and no extra sextupole families are needed. Since the octupoles are sufficient for the control of the footprint shape, less elements can be used ($G = 34$). However, by using the least possible elements or

ISBN: 978-3-95450-184-7 doi:10.18429/JACoW-IPAC2018-THPAF059

by increasing the non-linear families in a reduced lattice with a fixed G value, the strength of the non-linear kick is getting larger. As a consequence the non-linear perturbations are amplified.

In order to see what are the main resonances appearing in the effective lattice and if they are the same with the ones in the target lattice, frequency map analysis (FMA) is employed. Being interested in the dynamics of the particles at large amplitudes ($\sigma > 7$), initial conditions pf up to 10σ are taken. For these studies, a lattice with 2 sextupole families and $G = 130$ is used. The tune diffusion seen in the next plots is calculated according to the formula $Log_{10}[\sqrt{(Q_{X_f} - Q_{X_i})^2 + (Q_{Y_f} - Q_{Y_i})^2}]$ where, Q_i is the tune at the first 5000 turns and the Q_f is the tune calculated from the next 5000 turns [6]. As observed in Fig. 2, all the significant resonances that appear in the target lattice, Fig. 2a at flat bottom and Fig. 2c at flat top, play the same crucial role in the effective lattice Figs. 2b, 2b. For the particles at large amplitudes where the nonlinearities are stronger, there is some discrepancy. However, the footprint shape does not develop any strong deformation, especially at flat top energies.

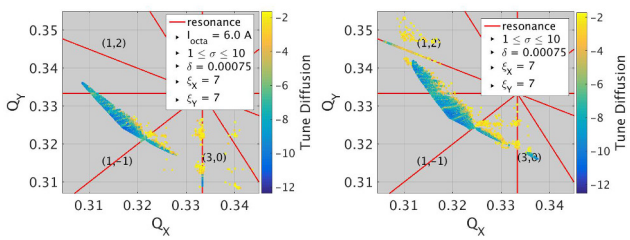

(a) Full lattice - flat bottom (b) Reduced lattice - flat bottom

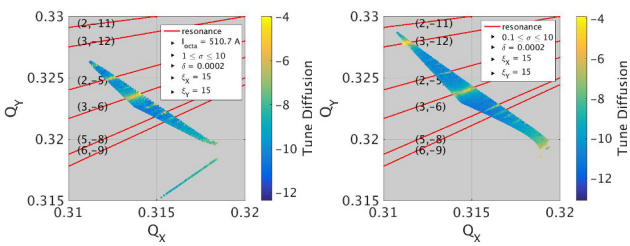

(c) Full lattice - flat top (d) Reduced lattice - flat top

Figure 2: Frequency maps of the full lattice and the reduced ones, at flat bottom (450 GeV) and flat top (6.5 TeV) energies

In order to better understand the dynamics of the particles at large amplitudes, dynamic aperture (DA) studies are performed and presented in Fig. 3. The DA values are obtained from tracking studies of one million turns. The tracking investigations for the target lattice are performed with SixTrack [7]. The results for the full and reduced lattice are plotted with red and black lines, respectively. At flat top energies (see Fig. 3b), a perfect reproduction of the minimum DA is achieved and the agreement with the target line (red) for different initial conditions (X_i and Y_i) is good. At flat bottom energies Fig. 3a, even if the reproduction of the minimum DA is not as accurate as for the flat top case, it is close to the target value. In general, the LHC at flat bottom energies suffers more from nonlinearities as observed in Figs. 2b, 2d. This makes even more difficult the task for the reduced lattice to reproduce the machine properties, at these energies.

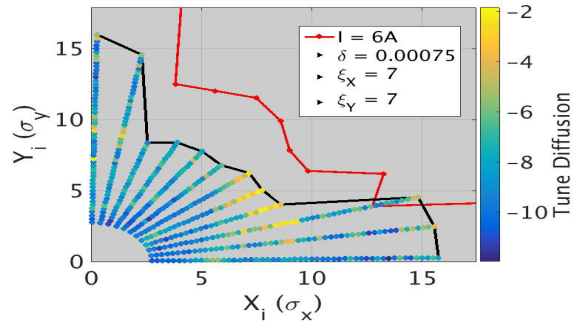

(a) Flat bottom

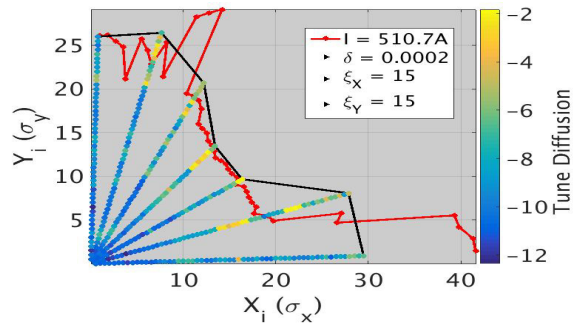

(b) Flat top

Figure 3: Dynamic aperture studies at flat bottom and flat top energies. With red lines are the results from the full lattice and with the black one the results from the reduced lattice.

CONCLUSION

It is well known that the task of reproducing the properties of a complicated non-linear system with a simplified alternative one is quite difficult. Having that in mind, the method presented above for the construction of an effective non-linear lattice has a very good agreement with the target quantities. The method is quite flexible to be used for any machine. It is ideal for studies that require fast multi-particle tracking and that comonly use simple linear rotations without taking into account the significant contribution of the machine nonlinearities.

REFERENCES

[1] J. Laskar and P. Robutel, “High order symplectic integrators for perturbed Hamiltonian systems", Celestial Mechanics and Dynamical Astronomy, 80(1), pp.39-62, 2001.

[2] K. Skoufaris, C. Skokos, Y. Papaphilippou and J. Laskar, "A benchmark study of a high order symplectic integration method with only positive steps", presented at the 9th Int. Particle

ISBN: 978-3-95450-184-7 doi:10.18429/JACoW-IPAC2018-THPAF059

Accelerator Conf. (IPAC'18), Vancouver, British Columbia, Canada, paper MOAB01, this conference.

[3] H. Goldstein, C. P. Poole and J. Safko, "Classical mechanics", San Francisco, Calif: Addison Wesley 2009.

[4] http://mad.web.cern.ch/mad

[5] A. Wolski "Beam dynamics in high energy particle accelerators", London: Imperial College Press, 2014

[6] Y. Papaphilippou, "Detecting Chaos in Particle Accelerators through Frequency Map Analysis Method", Chaos 24, 024412, 2014.

[7] http://sixtrack.web.cern.ch/SixTrack